Mass Lesion Detection with a Fuzzy Neural Network

H. D. Cheng and Muyi Cui

Dept. of Computer Science
Utah State University
Logan, UT 84322-4205, USA

ABSTRACT

This paper presents a novel fuzzy neural network (FNN) approach to detect malignant mass lesions on mammograms. The mammograms were obtained from the digital database for screening mammography (DDSM) at the University of South Florida. Six-hundred-seventy regions of interest (ROIs) were extracted from 100 mammograms and are randomly divided into two groups: training and testing sets. Entropy, uniformity, contrast, and maximum co-occurrence matrix elements are calculated at sizes of 256×256 and 768×768, respectively. The differences of these features (feature differences) from these two image sets with the above mentioned sizes are computed for each feature, and they are discriminant in differentiating between malignant masses and normal tissues regardless of lesion shape, size, and subtlety. After training, the FNN can correctly detect all malignant masses on mammograms in the testing group. The true positive fraction (TPF) is 0.92 when the number of false positives (FP) is 1.33 per mammogram; and 1.0 when the FP is 2.15 per mammogram.

1. INTRODUCTION

Breast cancer is one of the most prevalent cancers among women and is the leading cause of death for women in the age group of 15 to 54 [1]. One out of eight women will develop breast cancer during her lifetime in US. Mammography is one of the most effective tools in early detection of breast cancers [2]. Although significant progress has been made in breast cancer control by periodic mammogram screening, a considerable number of lesions are still missed due to a variety of factors including poor image quality, benign appearance of lesions, eye fatigue factor, and oversight of radiologists [3]. Mass lesions can be of different types and shapes, and the size varies from 1mm to several centimeters [4]. The presence of other structures makes the image background very complex for human and machine to distinguish malignant mass lesions from normal breast tissues.

Numerous attempts have been made to detect mass lesions on mammograms, such as image enhancement and template-matching techniques [5]; fuzzy pyramid linking algorithm [6]; and nonlinear bilateral subtraction technique [7]. These approaches require breasts to be symmetrical or lesions with typical shape. The presence of cancer causes the disturbance in the homogeneity of tissues and can result in architectural distortions in the surrounding breast parenchyma. As a result, texture measures of mammograms may be used as mass classification features. Local edge characteristics and textural features are used to identify spiculated masses [8]. By using statistical features from pairs of breasts, an area (A_z) under the receiver operating characteristics (ROC) curve of 0.823 was achieved [9]. A sensitivity of 92% for isolating malignant masses at 1.8 false positives per image was reported [11]. Fuzzy neural networks (FNN) provide a new way to interpret vague and incomplete data or knowledge. A fuzzy system adaptively infers and modifies its fuzzy associations from representative samples. Fuzzy logic based system can handle, to a reasonable extent, uncertainties in various applications, particularly in decision-making process under different kinds of risk, subjective judgment, vagueness, and ambiguity [10]. Image background can be of fuzzy nature because of the presence of some fatty tissues and blood vessels. In this paper, we will study a new set of features for the detection of mass lesions and studied the feasibility of using a FNN in the detection/classification process.

2. MATERIALS AND METHODS

Mammograms were downloaded from the DDSM. The mammograms were obtained with DBA M2100 ImageClear scanner. Sampling rate of the scanner was 42 microns per pixel. Gray level was 16 bits. Downloaded files were converted to gray level of 8 bits. Sub-images with sizes 128 × 128, 256 × 256, 512 × 512, 768 × 768, 1024 × 1024, and 1280 × 1280 were obtained as the regions of interests (ROIs) from each mammogram. For mammograms with malignant masses, all ROIs enclosed or overlapped the mass lesions. The ROIs were used to

study the effect of sample image size on texture features. The regions containing only normal tissues were also extracted randomly. Five to seven regions were selected from each mammogram. Two sample images were obtained from each of these regions with sizes 256 × 256 and 768 × 768, respectively. The sample image with size 256 × 256 p enclosed the whole small mass lesion or part of the large lesion. The sample image with size 768 × 768 enclosed the small image and its surrounding area. Entropy (E), uniformity (U), contrast (ν), and maximum co-occurrence matrix element were calculated for each ROI.

Texture features were computed for each ROI and fuzzified as the inputs of the fuzzy neural network. Based on co-occurrence matrix, entropy (E), uniformity (U), and contrast (ν) and maximum co-occurrence matrix element (CM_{max}) were computed.

2.1. Co-occurrence Matrix (CM) and Features

Grey-level co-occurrence matrix was calculated from angular matrices [14]. $P_{\theta,d}$ is the angular matrix at θ degrees (0^o, 45^o, 90^o, 135^o) and calculated for a distance of d between two pixels; a and b are the gray levels for these two pixels (k,l) and (m,n). The sum of the four angular matrices is expressed as:

$$p_d(a,b) = [p_{0^o,d} + p_{45^o,d} + p_{90^o,d} + p_{135^o,d}] \quad (1)$$

The co-occurrence matrix (C_{ij}) is calculated by dividing P_d by the total number of pixel pairs in the P_d calculation. In this research, d = 1 is used for the co-occurrence matrix calculation. Follows are the features extracted from CM.

2.2.1 Maximum co-occurrence matrix element (CM_{max})

$$CM_{\max} = \max_{i,j}(c_{ij}) \quad (2)$$

where c_{ij} is an element of the co-occurrence matrix (C_{ij}).

2.2.2. Contrast (ν)

$$v = \sum_i \sum_j (i-j)^2 c_{ij} \quad (3)$$

where c_{ij} is an element of the co-occurrence matrix (C_{ij}).

2.2.3. Entropy (E)

$$E = -\sum_i \sum_j c_{ij} \log c_{ij} \quad (4)$$

where c_{ij} is an element of the co-occurrence matrix (C_{ij}).

2.2.4. Uniformity (U)

$$U = \sum_i \sum_j c_{ij}^2 \quad (5)$$

where c_{ij} is an element of the co-occurrence matrix (C_{ij}).

2.3. Structure of the Fuzzy Neural Network

A four-layer feed-forward fuzzy neural network is used in this study. The first layer is the input layer consisting of 4 neurons. All features are normalized. The neurons in this layer are regular neurons.

$$s_i^{[2]} = \sum_{j=0}^{m-1} y_j^{[1]} w_j \quad (5)$$

$$\text{where } w_j = \begin{cases} \beta r_j & \text{i} \neq \text{j} \\ r_j & \text{i} = \text{j} \end{cases}$$

where β is the fuzzification coefficient. The value of $\beta \in [0,1]$ is determined experimentally, and r_j is the relative coefficient.

The output from the second layer is used to calculate the input values for the third layer. Neurons in the third layer are the maximum fuzzy neurons.

$$s_{ij}^{[3]} = \begin{cases} 1 - 2|\, y_j^{[2]} - \theta_i \,|/\alpha_i & \text{if } \alpha_i / 2 \geq |\, y_j^{[2]} - \theta_i \,| \geq 0 \\ 0 & \text{otherwise} \end{cases} \quad (6)$$

The number of fuzzy neurons in the third layer is determined during the training process. Each neuron in this layer represented a unique separable mass lesion pattern. The training algorithm determines α and θ for each fuzzy neuron. There are N fuzzy neurons in this layer. These neurons are divided into two classes: positive malignant mass lesion class (Mass) and normal tissue class (Normal). The maximum output from each class is obtained in the fourth layer and used as an input for a competitive neuron in the fourth layer.

The output function for the third layer is expressed as:

$$y_{c,i}^{[3]} = \max_{j=0}^{N-1}(s_{ij}^{[3]}) \quad (7)$$

where $y_{c,i}$ is the output of a fuzzy neuron in the third layer. The subscript c represents class index. If c is 0, it is the normal tissue class. If c is 1, it is the mass lesion class. The fourth layer has two maximum neurons and one competitive neuron with two inputs.

$$\begin{aligned} s_0^{[4]} &= \underset{i=0}{\overset{k}{Max}}(y_{c,i}^{[3]}) \\ s_1^{[4]} &= \underset{j=0}{\overset{l}{Max}}(y_{c,j}^{[3]}) \end{aligned} \quad (8)$$

where s_0 and s_1 are inputs to the competitive neuron. There are k neurons for malignant mass lesion class (Mass) and l neuron for normal class (Normal). The output of the fourth layer is defined as:

$$y^{[4]} = \begin{cases} 1 & \text{if } (s_0^{[4]} - s_1^{[4]}) \geq T_f \\ 0 & otherwise \end{cases} \quad (9)$$

where T_f is the activation threshold of the competitive neuron. If y equals one, it indicates that there is a malignant mass lesion.

2.4. Network Training

A set of inputs is applied to neurons in the first layer. The fuzzified output from each neuron in the first layer is fed to neurons in the second layer, where the sum is obtained after multiplied by respective weights and a fuzzification factor, and generated the output. Outputs from the second layer are fed to all FNN neurons in the third layer. If there is not a match with an existing class, create a new neuron with a defaultα. The maximum outputs from the third layer for each class are obtained in the fourth layer. After adjusting the decision threshold (T_V), a class is chosen. If misclassified, adjust α for that misclassified neuron; also create a new neuron for the new pattern with the minimum input as the parameterθ. Register the new neuron's index in the correct class. Re-train the neural network. Repeat these steps until all training sets are applied without requesting any weight modification.

3. RESULTS AND DISCUSSION

Entropies were 67% and 60% greater for ROIs with malignant mass than the ROIs with normal tissues at size of 128 × 128, 256 × 256 pixels, respectively (Fig. 1).

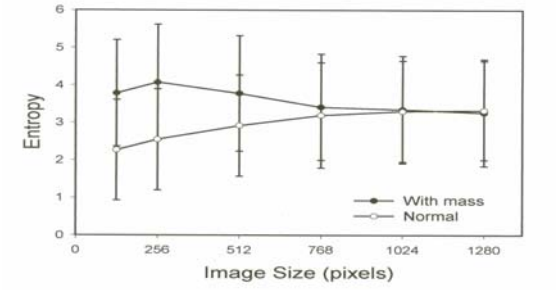

Fig. 1. Entropy (E) versus ROI size. Data are means ± standard deviations 52 ROIs with malignant masses (Mass) 44 normal ROIs (Normal).

Uniformities of ROIs with normal tissues were greater than those of ROIs with malignant masse with sizes of 128 × 128 and 256 × 256 (Fig. 2). It was similar for all ROIs with sizes of 768 × 768 and above. Contrast showed a similar pattern as for entropy (Fig. 3). Entropy difference was calculated by subtracting entropy of 768 × 768 from the one of 256 × 256. Entropy difference was greater for smaller lesions than that of lesions than that for larger lesions (Fig. 4). The contrast difference showed similar pattern (Fig. 5).

The entropy difference was positive for images with malignant masses while it was negative for normal images (Fig. 6). Contrast difference showed similar pattern as for entropy difference. The performance of the FNN was evaluated by the curve of a free-response receiver operating characteristic (FROC) [11]. The true positive fraction was plotted against the number of false positives per mammogram (FP) (Fig. 7). TPF was computed as TP/ (TP+FN). The TP is the number of true positives and FN is the number of false negatives. The number of FP per mammogram is 1.33 at a TPF of 0.92 and 2.15 at TPF 1.

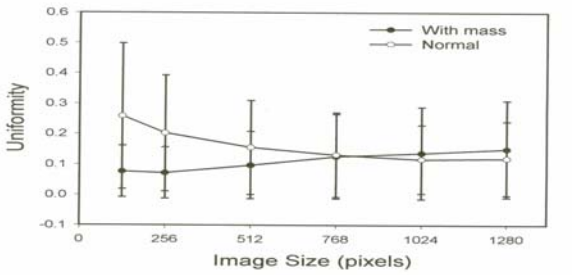

Fig. 2. Uniformity (U) versus ROI size. Data are means ± standard deviations 52 ROIs with malignant masses (Mass) and 44 normal ROIs (Normal).

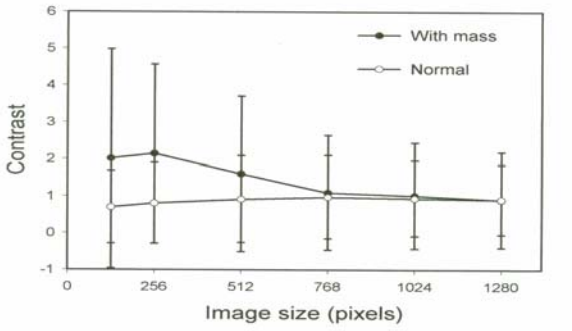

Fig. 3. Contrast (ν) versus ROI size. Data are means ± standard deviation for52 ROIs with malignant masses 44 normal ROIs.

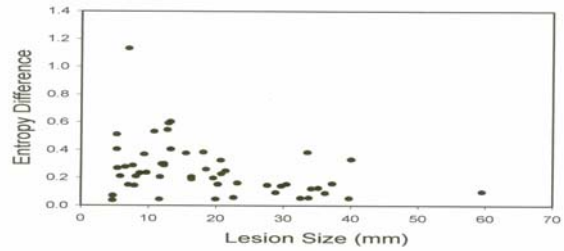

Fig. 4. Entropy difference (ΔE) versus lesion size of malignant masses. A total of 52 malignant masses are shown. The lesion size is calculated as $(a \times b)^{1/2}$. The variables a, b are the long and short axes of a malignant mass lesion, respectively. Entropy difference is calculated as $(E_{256} - E_{768})/ E_{768}$.

Some of these false positives could be benign masses in mammograms. The above result is better than most

published approaches for mass detection [7],[9], [12], [13].

The texture features used in this study appear to be very promising in distinguishing ROIs with malignant masses from those with normal tissues. Although a false positive of 2.15 per mammogram may not be adequate to be used as a primary tool for the detection of mass lesions, this classifier identified all malignant masses and can be used as a new assistant tool for radiologists for pre-screening of potential positive areas. Other modifications

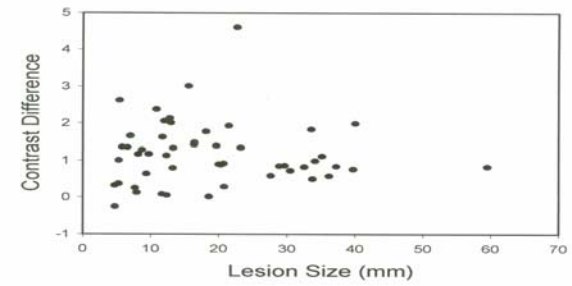

Fig. 5. Contrast difference (Δv) versus lesion size of malignant masses.

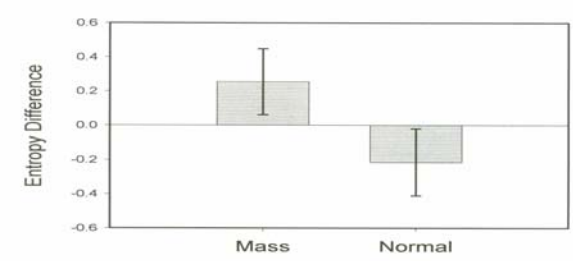

Fig. 6. Entropy difference (ΔE) for ROIs with malignant masses (Mass) and normal tissues (Normal). The error bars are standard deviations. For malignant masses, the number of samples is 52. The number of samples is 618 for normal tissues.

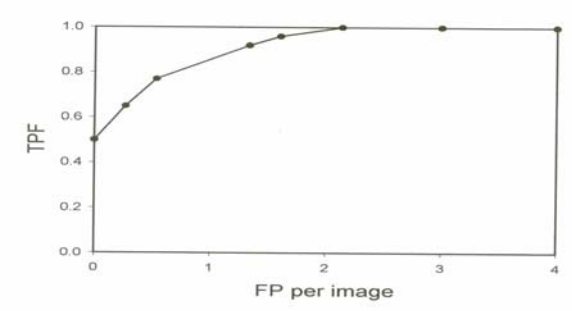

Fig.7. Free-response receiver operating characteristic (FROC) for the fuzzy neural network. The curve was obtained by adjusting the decision parameter in the fourth layer. True-positive fraction is computed as TP/(TP+FN), where TP is the number of true positives and FN is the number of false negatives (malignant mass lesions classified as normal tissues). FP is the number of false positives.

4. REFERENCES

[1] C.C. Boring, T.S. Squires, T, Tong, and M. Montgomery, "Cancer statistics, 1994," *CA-A Cancer J. for Clinicians*, vol. 44, pp. 7-26, 1994.

[2] H.C. Zuckerman, "The role of mammography in the diagnosis of breast cancer." In *Breast Cancer, Diagnosis and Treatment*, I. M. Ariel and J. B. Clear, Eds, New York: McGraw-Hill, 1987, pp.152-172.

[3] R.E. Bird, T.W. Wallace, and B.C. Yankaskas, "Analysis of cancer missed at screening mammography," *Radiol*., vol. 184, pp. 613-617, 1992.

[4] H. Li, Y. Wang, K.J. R Liu, S.B. Lo, and M.T. Freedman, "Computerized radiographic mass detection – Part I: Lesion site selection by morphological enhancement and contextual segmentation," *IEEE Trans. Med. Imaging*., vol. 20, pp. 289–301, 2001.

[5] S.M. Lai, X. Li, and W.F. Bischof, " On techniques for detecting circumscribed masses in mammograms," *IEEE Trans. Med Imaging*., vol. 8, pp. 377-386, 1989.

[6] D. Brzakovic, X.M. Luo, and P. Brzakovic, "An approach to automated detection of tumors in mammography," *IEEE Trans. Med. Imaging*., vol. 9 pp. 233-241, 1990.

[7] F.–F. Yin, M.L Giger, K. Doi, C.E. Metz, C.J. Vyborny, and R. A. Schmidt, "Computerized detection of masses in digital mammograms: Analysis of bilateral subtraction images," *Med. Phys*. Vol. 18, pp. 955-961, 1991.

[8] W. P. Kegelmeyer, J. M. Pruneda, P. D. Bourland, A. Hillis, M. W. Riggs, and M. L. Nipper, " Computer-aided mammographic screening for spiculated lesions," *Radiol*., vol. 191, pp. 331-337, 1994.

[9] H.–P. Chan, D. Wei, M. A. Helvie, B. Sahiner, D. D. Adler, M. M. Goodsitt, and N. Patrick, " Computer-aided classification of mammographic masses and normal tissue: Linear discriminant analysis in texture feature space, " *Phys. Med. Biol*., vol. 40, pp. 857-876, 1995.

[10] S.K. Pal and S. Mitra, *Neuro-fuzzy pattern recognition methods in soft-computing*. New York, NY: Wiley, 1999.

[11] C.E. Metz, "ROC methodology in radiologic imaging," *Investigative Radiology*, vol. 21, pp. 720-733, 1986.

[12] A. Mendez, P. Tahoces, M. Lado, M. Souto, J. Vidal, "Computer-aided diagnosis: Automatic detection of malignant masses in digitized mammograms," *Med. Phys.*, vol. 25, pp. 957–964, 1998

[13] N.R. Mudigonda, R.M. Rangayyan, and J.E.L. Desautels, "Gradient and texture analysis for the classification of mammographic masses," *IEEE Trans. Med. Imaging*, vol. 19, pp. 1032–1043, 2000.

[14] R. Jain, R. Kasturi, and B.G. Schunck, *Machine Vision*. New York, NY: McGraw-Hill, Inc., 1995